Detection of ULF Geomagnetic Anomalies Prior to the Tohoku-Oki Earthquake by the Multireference Station Method

Jiyan Xue, Qinghua Huang, Sihong Wu, and Li Zhao

***Abstract*— The ultralow-frequency (ULF) electromagnetic anomaly has been considered one of the earthquake precursory signals with the potential for short-term prediction. As such, effectively detecting ULF anomalies is important for mitigating earthquake disasters. Given the comprehensive coverage of geomagnetic networks in Japan, the 2011 Tohoku-Oki earthquake (M9.0) provided a tremendous opportunity for investigating the characteristics and mechanisms of ULF anomalies. Previous studies reporting detections of ULF anomalies triggered by the Tohoku-Oki earthquake have been questioned on the grounds of insufficient reliability due to technological limitations. In this study, we employ a multireference station data-quality-weighted method to detect the ULF anomaly. Comparison with traditional single-reference station method demonstrates the robustness of our detection results. A statistical test also indicates that the ULF anomaly appearing approximately two months before the earthquake was driven by physical processes. Geomagnetic storm analysis further rules solar activity as the cause of the anomaly. The spatial distribution of the anomaly amplitude reveals a decrease in the anomaly energy with increasing epicentral distance, implying a strong association between the anomaly and the earthquake. Our study is helpful for understanding the possible connection between the ULF electromagnetic precursors and the seismogenic processes of strong earthquakes, which contributes to achieving the ultimate goal of short-term earthquake prediction.**

***Index Terms*— Multireference stations (MRSs), seismo-electromagnetism, Tohoku-Oki earthquake, ultralow-frequency (ULF) phenomena.**

I. Introduction

EARTHQUAKES are one of the most devastating types of natural disasters and can be accompanied by secondary hazards such as mudslides, landslides, and tsunamis, leading to devastating hazards to human lives and properties [1], [2], [3]. Exploring short-term earthquake prediction capabilities based on reliable precursors is the most direct and effective approach to mitigating earthquake disasters but also the most challenging research field [4], [5]. During the seismogenic stage, with the increase in stress, the accumulated energy may disturb the geophysical fields and give rise to precursory anomalies [6], [7]. At present, widely reported precursor phenomena include seismic electric signals (SESs) [8], [9], [10] and their activities [11], [12], [13], [14], [15], seismomagnetic phenomena [16], [17], thermal infrared radiations [18], [19], [20], and seismic activities [21], [22], [23], [24]. Among these, seismo-electromagnetic signals, whose existence and applicability have been confirmed statistically, are regarded as the most promising type of precursor for achieving breakthroughs in short-term earthquake prediction [17]. Therefore, over the past two decades, researchers have increasingly focused on extracting precursory signals from electromagnetic observations, driving the continuous development of seismo-electromagnetism [25].

There have been numerous reports of pre-earthquake ultralow-frequency (ULF) geomagnetic anomalies [17], [26]. Due to the complex nature of the energy sources of geomagnetic data and the relatively weak energy induced by the seismogenic process, these reports typically combined various signal processing techniques to extract meaningful anomalies from the background geomagnetic field. Fedi et al. [27] utilized continuous wavelet transform singular analysis and time-varying statistical analysis, to reveal a strong correlation between geomagnetic anomalies and volcanic as well as fault activities. Hattori et al. [28], Han et al. [29], and Huang [30] applied a principal component analysis to detect geomagnetic anomalies and observed heightened energy in the second principal component before multiple seismic events in Japan and China. Hattori et al. [31] and Han et al. [32] conducted superposed epoch analysis to confirm the existence of ULF seismomagnetic phenomena preceding major earthquakes, which contributes to enhancing the accuracy of short-term earthquake prediction. Febriani et al. [33] employed wavelet transform and detrended fluctuation analysis and discovered a significant increase in spectral density ratio within a specific frequency range of the geomagnetic signals preceding major earthquakes. Han et al. [34], [35] utilized Molchan's error diagram to demonstrate that ULF anomalies can effectively enhance the accuracy of short-term earthquake predictions. Heavlin et al. [36] used spectral cross-power to verify the anomalies in the geomagnetic data preceding 19 earthquakes ($M \geq 4.5$) in California. Yusof et al. [37] employed superposed epoch analysis to investigate the global ULF precursor phenomena and demonstrated that their appearance is statistically significant rather than coincidental.

The pioneering study of Hattori [38] provided a quantitative relationship between the detectable range of ULF anomalies triggered by earthquakes and their magnitudes.

Manuscript received 21 January 2024; revised 14 March 2024; accepted 24 March 2024. Date of publication 27 March 2024; date of current version 4 April 2024. This work was supported by the National Natural Science Foundation of China under Grant U2239201 and Grant 42021003. *(Corresponding author: Qinghua Huang.)*

The authors are with the Department of Geophysics, School of Earth and Space Sciences, Peking University, Beijing 100871, China (e-mail: xjy2001110580@stu.pku.edu.cn; huangq@pku.edu.cn; sihongwu@pku.edu.cn; lizhaopku@pku.edu.cn).

Digital Object Identifier 10.1109/TGRS.2024.3382472

The 11 March 2011 Tohoku-Oki earthquake (M9.0) off the northeast coast of Japan was extensively observed by the geomagnetic observatories in Japan, ensuring stable and consistent data collection [39]. The occurrence of this major earthquake event and the comprehensive dataset present a rare opportunity to investigate the characteristics and mechanisms of the ULF geomagnetic phenomena.

Some precursory phenomena related to the Tohoku-Oki earthquake have been reported. For example, Orihara et al. [40] found that the water level and temperature from wells approximately 155 km away from the epicenter showed anomalous decrease three months before the earthquake; Nagao et al. [41] reviewed geodetic, electromagnetic, and ionospheric anomalies; Sarlis et al. [42] conducted natural time analysis (NTA) and found the deepest minimum in the fluctuation of the order parameter of seismicity approximately two months before the earthquake; Varotsos et al. [43] used the pressure stimulated polarization current model to explain various geophysical precursory phenomena; and Varotsos et al. [44] combined NTA with nonextensive statistical mechanics and shortened the time window of the impending earthquake from a few days to several hours.

Xu et al. [45] and Han et al. [46], [47] studied the ULF geomagnetic phenomena before the Tohoku-Oki earthquake. However, the single-reference station method employed in their studies implies that their conclusions were dependent upon the same specific reference station, and the effect of the reference station was not investigated. In addition, subsequent discussion results in this article indicate that relying solely on a single-reference station affects the reliability and robustness of anomaly detection and reduces the capacity to effectively extract the potential characteristics and mechanisms of the ULF anomalies.

In this study, we apply a multireference station (MRS) data-quality-weighted method, combined with statistical tests as well as solar activity and spatiotemporal analysis, to systematically investigate the characteristics and mechanisms of the ULF anomaly associated with the 2011 Tohoku-Oki earthquake. We first examine the criteria for the reference and target stations so that the data satisfy the requirement on the temporal and spatial extent, followed by an introduction to the geomagnetic data preprocessing techniques and the MRS data-quality-weighted method. Next, we compare our proposed method with the traditional single-reference station method to show that our approach achieves higher stability in ULF anomaly detection. Then, we carry out a significance test to demonstrate the robustness of our result and a global geomagnetic storm analysis to exclude solar activity as a possible cause of the detected ULF anomaly. We also examine the spatial variation of the ULF anomaly amplitude, which exhibits an apparent association of the anomaly with the location of the Tohoku-Oki earthquake.

II. Data

In this section, we identify the reference and target stations utilized in the study. An accurate understanding of the physics of the geomagnetic diurnal variation field (GDVF) is important for anomaly detection and the appropriate selection of stations. The GDVF primarily comprises two components: external and internal [48], [49]. The external field originates from disturbances in the spatial current system caused by solar activity, constituting the primary component of the GDVF. Because of the global-scale impact of solar activity, the external field typically exhibits strong coherence across larger distances, with similarities in external fields at stations located hundreds of kilometers away. The internal field refers to the induced magnetic field originating from the conductive Earth, and its variation characteristics are closely related to the subsurface electrical structure. Therefore, the main reason for the differences in observations among different stations is the alterations in the internal fields caused by the unique electrical structures at each station. Theoretically, the GDVF difference between stations would remain stable as long as the electrical structures beneath all stations are the same. However, the seismogenic process alters the electrical structures beneath stations near the epicenter, disrupting the stability of the GDVF difference and causing anomalies in the internal fields.

We aim to detect the precursory ULF anomalies by utilizing the anomalies in the GDVF differences between the reference and target stations. Therefore, the selection of reference stations must meet two necessary conditions.

1) Sufficiently far from the epicenter so that local anomalies resulting from the seismogenic process do not affect the reference stations.
2) Certain distance from the target stations to ensure similarity in the external field among the stations, thus highlighting the internal field anomalies.

We use the detectable range of ULF anomalies proposed by Hattori [38] and the introduction of the Earth's magnetic field by Lanza and Meloni [49] to define the selection range for target and reference stations

$$R_{\mathrm{TS}} \leq \frac{M-4.5}{0.025}(\mathrm{km}) \tag{1}$$

$$\frac{M-4.5}{0.025} < R_{\mathrm{RS}} < R_{\mathrm{TS}} + R_{\max}(\mathrm{km}) \tag{2}$$

where R_{TS} and R_{RS} represent the epicentral distances of the target and reference stations, respectively; M is the magnitude of the earthquake; and $R_{\max}$ represents the maximum distance between the target and reference stations, i.e., condition (2) above. In this study, $R_{\max} = 600$.

In analyzing the precursors of the Tohoku-Oki earthquake, based on (1) and the distribution of geomagnetic stations in Japan, we choose the ESA station with an epicentral distance of 135.92 km as the target station (Fig. 1). Then, following the (2), we select SIK, HAG, KAK, OTA, and KNZ as reference stations. The distances from the reference stations to the target station (ESA) and the epicenter are computed, as listed in Table I. To investigate the ULF anomalies potentially triggered by the 2011 Tohoku-Oki earthquake, we analyze the data from 2009 to 2012.

III. Method

A. Z-Ratio Metric

Previous case studies on short-term earthquake prediction [32], [50], [51] have shown that the ratio of Z-component

TABLE I
DISTANCES FROM THE FIVE SELECTED REFERENCE STATIONS TO THE TARGET STATION (ESA) AND THE EPICENTER OF THE TOHOKU-OKI EARTHQUAKE

Reference Station	Distance from ESA (km)	Distance from epicenter (km)
SIK	467.05	511.16
HAG	514.39	526.04
KAK	349.08	300.23
OTA	448.28	383.98
KNZ	459.56	401.19

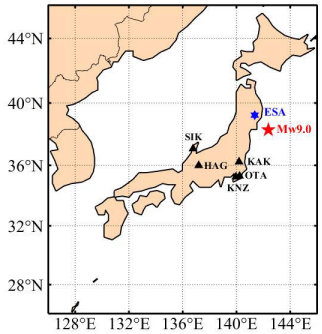

Fig. 1. Spatial distributions of the epicenter of the 2011 Tohoku-Oki earthquake (red star) and the selected reference (black triangles) and target geomagnetic stations (blue hexagon). The five reference stations are Shika (SIK), Hagiwara (HAG), Kakioka (KAK), Otaki (OTA), and Kanozan (KNZ). The target station is Esashi (ESA).

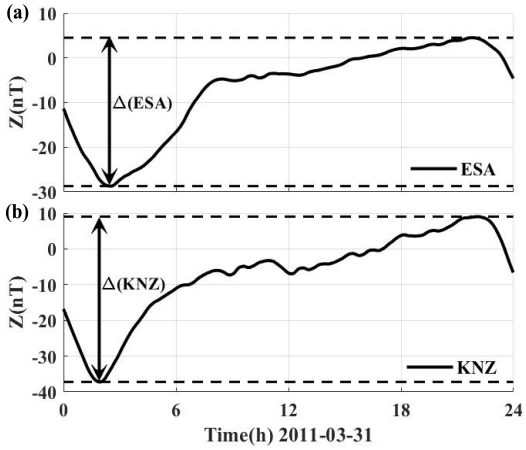

Fig. 2. Diurnal variations of Z-component ULF observations at stations (a) ESA and (b) KNZ, on March 31, 2011. ΔESA and ΔKNZ denote the diurnal variation ranges at the two stations.

diurnal variation ranges between the target and reference stations can be used as an effective metric for ULF anomalies. Fig. 2 shows the diurnal variations of ULF observations at the reference station KNZ and target station ESA used to detect the ULF anomaly.

The spectral analysis of the GDVF data (Fig. 3) indicates that the geomagnetic data are dominated by tidal energy with periods ranging from 24 h to several hours. These long-period baseline drifts are removed by a least-squares fitting based on a

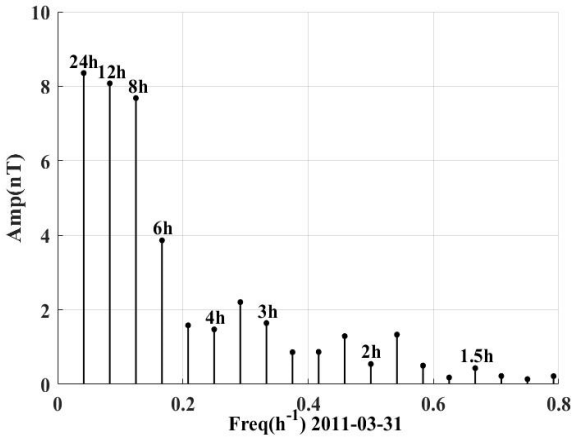

Fig. 3. Spectral analysis for the observation at station KNZ on March 31, 2011. The geomagnetic diurnal variation data are dominated by the tidal signals of periods exceeding 1.5 h.

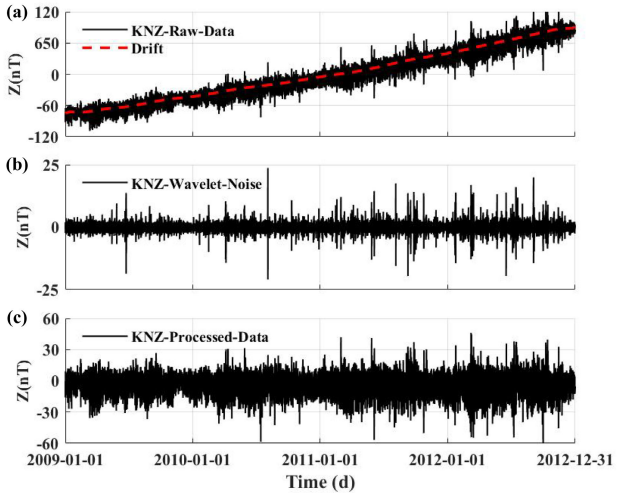

Fig. 4. Data processing for station KNZ. (a) Raw data (solid black line) and the long-term baseline drift based on least-squares polynomial fitting (red dashed line). (b) Noise of periods shorter than 64 min. (c) Processed data after removals of baseline drift and noise.

sixth-order polynomial [Fig. 4(a)]. In addition to the baseline drifts, relatively high-frequency noises (periods shorter than 64 min) in the data, which affect the accuracy of the estimation of diurnal variation range estimation, are suppressed by wavelet denoising based on the "db5" wavelet function [Fig. 4(b) and (c)]. The wavelet denoising [52] used in this study is consistent with that utilized by Han et al. [46], with detailed methodological specifics therein.

We employ the processed data for the KNZ and ESA stations to calculate the ratio of the Z-component daily variation amplitudes

$$Z - \text{Ratio}(\text{KNZ}, \text{ESA}) = \frac{\Delta\text{KNZ}}{\Delta\text{ESA}} \tag{3}$$

where ΔKNZ and ΔESA are the diurnal variation ranges at the two stations, as shown in Fig. 2. There are apparent long-term seasonal variations in the Z-Ratio [Fig. 5(a)]. To minimize the impact of seasonal disturbances, we utilize wavelet denoising again to remove noises with periods of six months and longer [Fig. 5(b)]. On the other hand, the

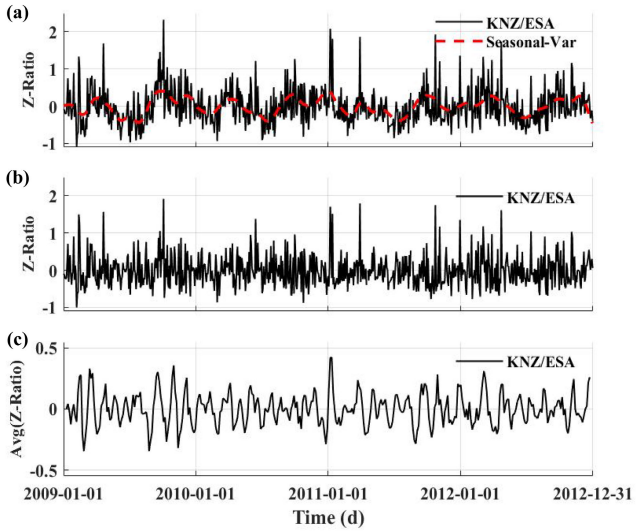

Fig. 5. Noise characteristics and denoising results of Z-Ratio for KNZ and ESA stations. (a) Ratio of Z-component daily variation amplitudes (solid black line) and seasonal disturbance noise with periods greater than six months (red dashed line). (b) Same as (a), but with seasonal disturbance removed. (c) Moving average ratio calculated using a 12-day-long moving window.

Z-Ratio is also prone to interference from the ionospheric currents induced by solar activity, leading to seemingly random fluctuations [Fig. 5(b)]. Fortunately, these disturbances induced by ionospheric currents typically last only a few days, whereas earthquake-induced anomalies persist for longer durations. Therefore, we calculate the moving average of the Z-Ratio using a 12-day-long moving window to suppress ionospheric current disturbance and highlight earthquake-induced anomalies [Fig. 5(c)].

B. MRS Data-Quality-Weighted Method

The reference stations differ from one another in terms of location, equipment, technology, and maintenance, which affects the accuracy and quality of the data [53]. Therefore, the stability and reliability of the results vary among different reference stations. We repeat the process in Section III-A to obtain the Z-Ratio results for the other four selected reference stations and quantitatively evaluate their quality. The evaluation results are used to weigh the Z-Ratios obtained from each reference station to achieve a more stable and robust detection result.

During the four-year observation period, data from each station suffered varying degrees of loss mainly due to various factors such as station maintenance problems, system failures, and communication interruptions [46]. Therefore, the extent of data loss and level of noise interference serve as metrics to evaluate the data quality. We define the data integrity rate (DIR) and signal-to-noise ratio (SNR) as

$$\mathrm{DIR} = \left(1 - \frac{D_{\mathrm{miss}}}{D_{\mathrm{total}}}\right) \times 100\% \tag{4}$$

$$\mathrm{SNR} = 10 \times \log_{10}\left(\frac{P_s}{P_n}\right) \tag{5}$$

where D_{miss} and D_{total} denote the number of days of missing data and the total number of days, respectively; and P_s and P_n are the average signal and noise powers, respectively. Table II lists the DIR and SNR values for the five reference stations.

TABLE II
DATA QUALITY EVALUATIONS AND WEIGHTS FOR THE FIVE REFERENCE STATIONS

Station	SIK	HAG	KAK	OTA	KNZ
DIR	90.01%	92.47%	100%	98.08%	99.86%
SNR	25.44	29.32	28.25	25.15	23.57
W	0.33	0.62	0.91	0.58	0.50

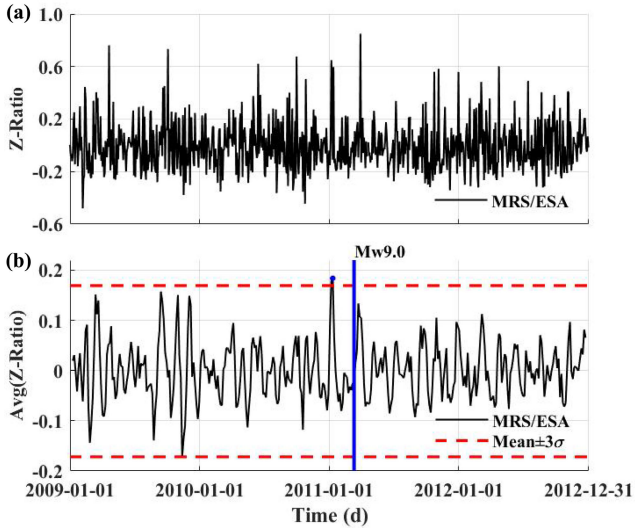

Fig. 6. Detection results using data-quality-weighted Z-Ratio. (a) Weighted MRS Z-Ratio obtained from the five reference stations. (b) 12-day moving average Z-Ratio obtained from (a). Red dashed lines represent the $\pm 3\sigma$ threshold, while the blue solid line marks the origin time of the Tohoku-Oki earthquake. The blue dot denotes the anomaly detected on 18 January 2011.

We use a linear function to determine the weights for the Z-Ratio

$$W_i^k = \frac{DQ_i^k - \min\left(DQ^k\right)}{\max\left(DQ^k\right) - \min\left(DQ^k\right)} \times \left(W_{\max} - W_{\min}\right) + W_{\min} \tag{6}$$

$$W_i = \prod_{k=1}^{\max}(k) W_i^k \tag{7}$$

where DQ_i^k represents the kth data quality metric ($k = 1$ and 2 for DIR and SNR) for the ith station ($i = 1, 2, \ldots, 5$). $W_{\max} = 1$ and $W_{\min} = 0.5$ represent the maximum and minimum values of the weights, respectively. The weighted MRS Z-Ratio [Fig. 6(a)] is obtained from the Z-Ratios and weights W_i at the five reference stations. Then, we calculate the moving average using a 12-day-long moving window and adopt 3σ as the threshold for anomaly detection [Fig. 6(b)].

IV. RESULTS AND DISCUSSION

The detection result depicted in Fig. 6(b) indicates that approximately two months before the 2011 Tohoku-Oki earthquake, there was a singular occurrence of anomalous Z-Ratio

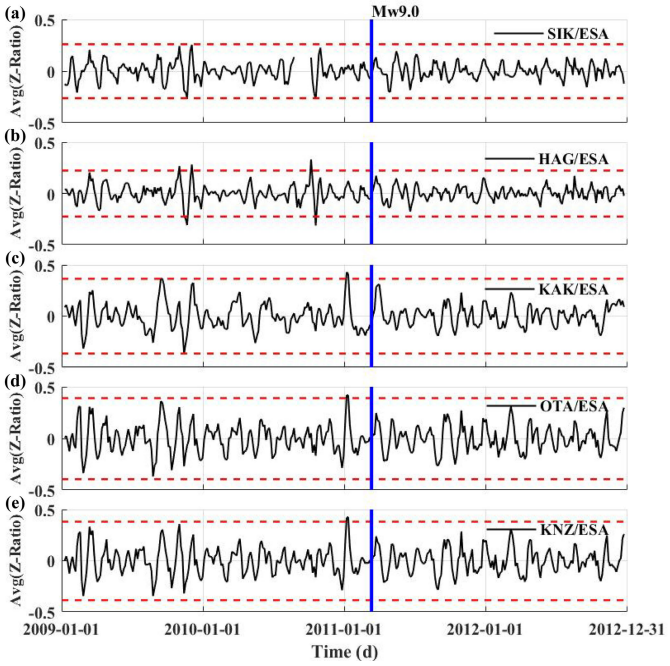

Fig. 7. Detection results using single-reference station. (a)–(e) Detection results using SIK, HAG, KAK, OTA, and KNZ individually as the reference station.

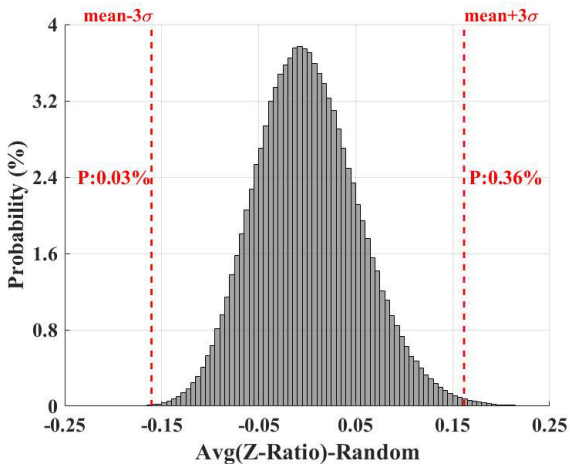

Fig. 8. Probability distribution of the averages of 500 000 random samples. The horizontal axis represents the 12-day average of the randomly selected Z-Ratios, and the red dashed lines mark the $\pm 3\sigma$ threshold for detecting anomalies. P: 0.03% and P: 0.36% represent the probabilities of exceeding the thresholds of -3σ and $+3\sigma$ as 0.03% and 0.36%, respectively.

exceeding the threshold against a relatively tranquil geomagnetic background over four years. The anomaly detected on January 18, 2011 was the most significant throughout the four-year observation period (with the largest amplitude). In this section, we assess the robustness of our detection result by significance test, geomagnetic storm analysis, and spatiotemporal feature studies and explore the potential mechanisms of this anomaly.

A. Comparison With Single-Reference Station Method

The traditional single-reference station method has a stronger reliance on the subjective selection of the reference station. Therefore, the random nature in reference station selection in traditional methods makes the obtained detection results unstable, leading to biases in the understanding about the characteristics or mechanisms of anomalies. In this section, we analyze the detection results of single-reference station to demonstrate this bias.

Fig. 7 illustrates the detection results using five individual reference stations satisfying the criteria in Section II. The results using SIK or HAG as reference station [Fig. 7(a) and (b)] show no anomaly according to the threshold of 3σ before the Tohoku-Oki earthquake. On the other hand, the results using one of the other three stations [Fig. 7(c)–(e)] draw a completely different conclusion, demonstrating that relying solely on a single-reference station leads to unstable results. In contrast, the MRS method combines the results obtained from individual reference stations with a data quality consideration, thus addressing the hyperparameter issue of reference station determination and resulting in a more robust and stable outcome.

B. Significance Test

Recently, researchers have proposed physical models to explain the electromagnetic precursory phenomena [43], [54]. Due to the limited physical understanding of the entire seismogenic process, we adopt a data-driven statistical approach to assessing the reliability of anomalies.

We follow the basic steps of significance testing, which include the following:

1) stating an assumption and setting the significance level (SL, typically set at 5%);
2) designing experiments and calculating probability distributions;
3) comparing the probability of the assumption occurring with the SL;
4) accepting or rejecting the assumption [45], [55].

"Rejecting the assumption when the probability is less than the SL" means that the probability of the assumption occurring is lower than the SL, so we should consider that statistically the assumption does not occur.

Specifically, we assume that the singular anomaly arises from random factors rather than a specific physical process and set the SL to 5%. We randomly retrieve 500 000 12-day-long samples from the Z-Ratio data and compute their averages. We analyze the probability distribution of the averages of the random samples and set a 3σ as the threshold (Fig. 8). The statistical results indicate that for a random case, the probability of detecting anomalies is only 0.39% (1950 times) (meaning that there is a 0.39% chance that an anomaly might occur due to random factors), lower than the SL of 5%. Therefore, this assumption should be rejected statistically, and the anomaly is not caused by random factors but controlled by an underlying physical process.

C. Geomagnetic Storm Analysis

The external field constitutes the primary component of the GDVF, allowing the diurnal variations to reflect the level of

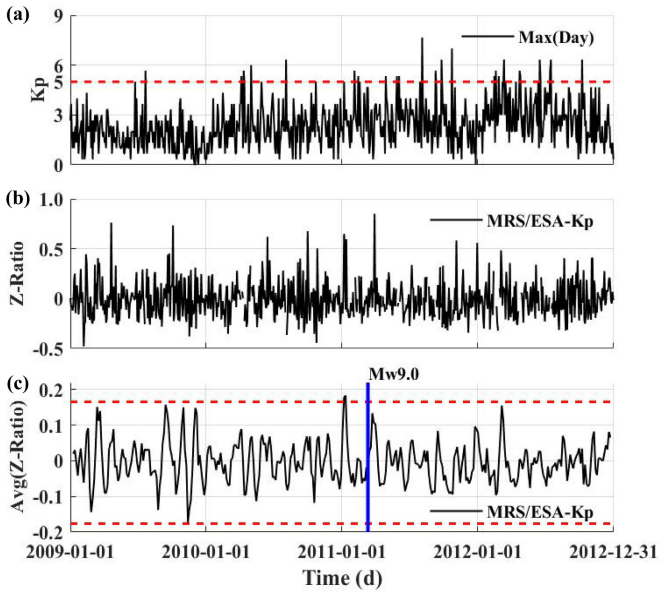

Fig. 9. Association analysis between global geomagnetic storms and the anomaly. (a) Maximum K_p values for each day from 2009 to 2012. The red dashed line represents geomagnetic storm events ($K_p \geq 5$). (b) Z-Ratio and (c) 12-day average after excluding the impact of geomagnetic storms.

solar activity with high sensitivity. The global geomagnetic storms, resulting from the interaction between high-energy charged particle streams generated by solar activity and the Earth's geomagnetic field, often lead to anomalies in the diurnal variations. Hence, it is essential to eliminate intense disturbances caused by solar activity before analyzing the correlation between any specific anomaly and an earthquake.

We use the geomagnetic K_p index to represent the level of solar activity and record the maximum K_p value for each day between 2009 and 2012 [Fig. 9(a)]. According to the geomagnetic storm intensity scale delineated by the Space Weather Prediction Center (SWPC) of the National Oceanic and Atmospheric Administration (NOAA), $K_p \geq 5$ indicates the occurrence of geomagnetic storms. During periods of geomagnetic storms, it is not feasible to analyze the correlation between anomalies and earthquakes. Therefore, we exclude the Z-Ratio data during stormy occurrences [Fig. 9(b)] and recalculate the 12-day moving average [Fig. 9(c)]. After excluding the geomagnetic storm impact, the anomaly appearing around two months before the Tohoku-Oki earthquake persists, indicating that this anomaly is unrelated to solar activity. The lead time of approximately two months agrees with the average lead time observed since the 1990s for various SES activities [12], [13], which have also been verified as unrelated to solar activity.

D. Spatial Variation of Anomaly Amplitude

In the previous discussion, we have demonstrated that the anomaly is statistically significant, arising from a physical process and independent of global geomagnetic storms. Here, we further explore the potential correlation between the anomaly's spatial variation and the location of the earthquake. Thanks to the full coverage of geomagnetic stations in Japan, we select nine additional target stations with a range of

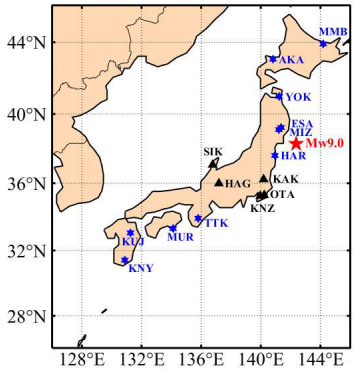

Fig. 10. Distribution of the nine additional target stations. They are in the order of increasing distance from the epicenter of the Tohoku-Oki earthquake, Mizusawa (MIZ), Haramachi (HAR), Yokohama (YOK), Akaigawa (AKA), Memambetsu (MMB), Totsugawa (TTK), Muroto (MUR), Kuju (KUJ), and Kanoya (KNY). Other symbols are the same as in Fig. 1.

epicentral distances from the Tohoku-Oki earthquake (Fig. 10). The duration of data used in this experiment remains consistent with the previously mentioned period.

With the newly selected nine target stations and the same five reference stations, we employ the same method as in Section III to obtain the detection results. It should be noted that the same threshold (3σ) leads to different values for different stations (e.g., the 3σ values for the MIZ and ESA stations are 0.13 and 0.17, respectively), which makes it difficult to compare the detection results. Therefore, we normalize the values obtained for different stations and scale the detection results for all stations. Fig. 11 shows the normalized detection results from 2010 to 2011 for nine target stations, where anomalies are detected approximately two months before the Tohoku-Oki earthquake. The anomalies detected on January 18, 2011 exhibit the largest amplitudes [Fig. 11(a)], consistent with the results in Fig. 6, leading us to select these anomalies for spatial feature analysis.

It is noteworthy that the anomalous date agrees remarkably well with the results independently obtained by Sarlis et al. [42] through NTA [15]. Sarlis et al. [42] indicated that the fluctuation of the order parameter of seismicity exhibited distinct minima several months before all shallow earthquakes of $M \geq 7.6$, with the deepest minimum occurring about two months before the M9 Tohoku-Oki earthquake. Furthermore, Varotsos et al. [15], [56] have also demonstrated that the minima of the order parameter of seismicity almost coincided with the initiation of the SES activities and exhibited spatial correlation. These analyses of multigeophysical data strongly support the credibility of the anomalies obtained in this study.

To fully understand the spatial variation characteristics of the anomaly, we plot in Fig. 12 the anomaly amplitudes of ESA and the nine new target stations as a function of their distances from the epicenter. Fig. 12 illustrates that despite fluctuations in the anomaly amplitudes at stations YOK and TTK, there is a clear decreasing trend of the anomaly amplitude with the increasing distance from the epicenter. In other words, the anomaly energy is well-concentrated at the epicenter of the Tohoku-Oki earthquake, strongly implying a correlation between the detected anomaly and the earthquake.

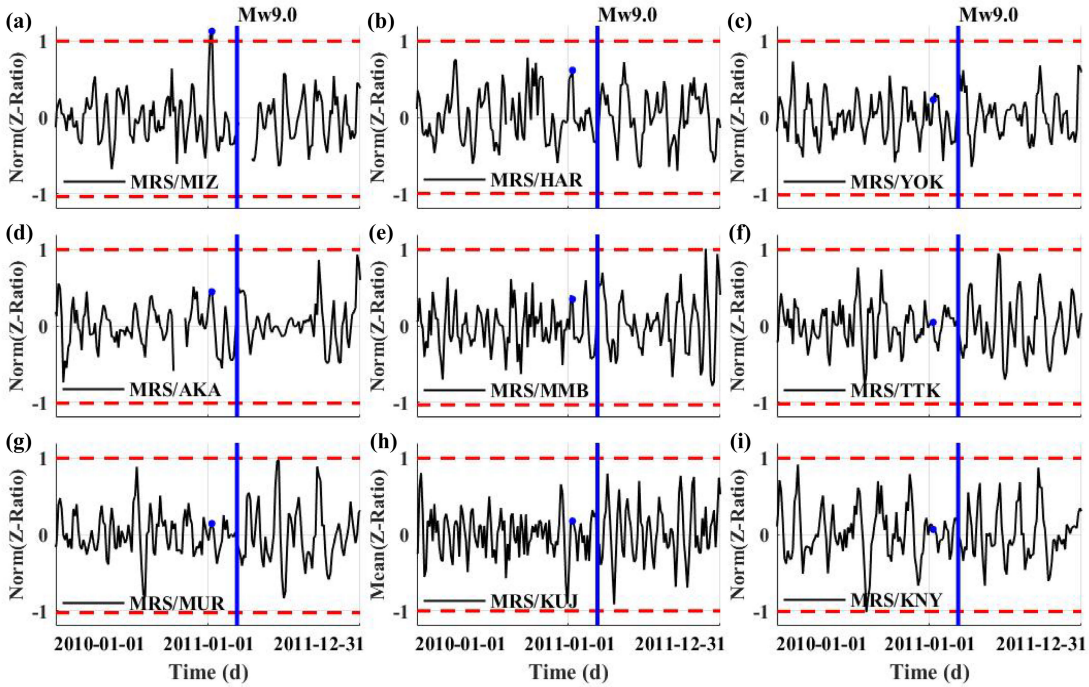

Fig. 11. Normalized detection results from 2010 to 2011 for nine target stations. The blue solid lines mark the origin time of the 11 March 2011 Tohoku-Oki earthquake, while the blue dots denote the detected anomalies on 18 January 2011. (a)–(i) Represent the detection results for the MIZ, HAR, YOK, AKA, MMB, TTK, MUR, KUJ, and KNY stations, respectively.

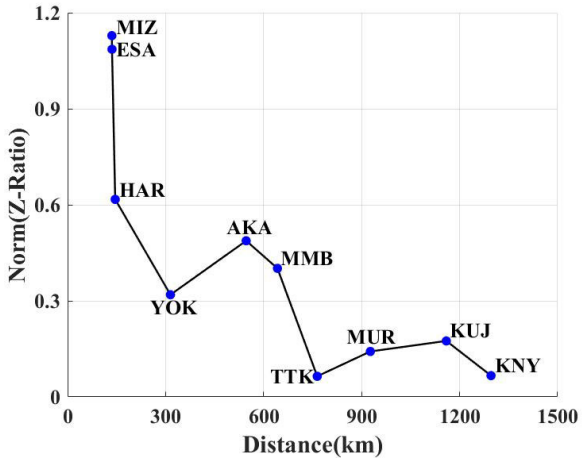

Fig. 12. Spatial decay of the detected anomaly energy with epicentral distance. The horizontal axis represents the distance between the target stations and the epicenter of the Tohoku-Oki earthquake, while the vertical axis represents the normalized anomaly amplitude as shown in Fig. 11.

Besides, the spatial variation characteristics of the ULF anomaly are consistent with the results obtained independently by Sarlis et al. [57] through NTA. Sarlis et al. [57] analyzed the spatiotemporal variations of the order parameter of seismicity for six shallow earthquakes of $M \geq 7.6$ recorded in Japan from 1984 to 2011. The results indicated that the epicentral locations depicted by spatiotemporal variations lie within a few hundred km of their actual epicenters.

E. Future Developments

In this study, we adopt the MRS method and employ the diurnal variation range ratio as the metric to investigate the potential of ULF phenomena as an earthquake precursor. This approach relies on the expert decision to select features conducive to characterizing the relevant precursory phenomena. However, due to the limited understanding of seismo-electromagnetic physics, manually selected features are prone to interference from other sources and may not effectively highlight the target anomalies. Therefore, even for the Tohoku-Oki earthquake, one of the largest earthquakes on record, identifying the ULF anomalies in the seismogenic phase is only achievable at ESA and MIZ, the two stations located sufficiently close to the epicenter.

Deep learning (DL) technique has the capability to automatically extract effective features from data, demonstrating an outstanding ability of representing nonlinear relationships [58], [59] and leading to widespread applications to geophysical problems [60], [61]. Compared to physics-based algorithms, data-driven DL methods have lower requirements in understanding the background physical processes of the problems, making them more applicable for studying the ULF precursor phenomena. Xue et al. [62], [63] employed deep neural networks to extract seismic electrical signals from geoelectric data influenced by severe railway noise and demonstrated the significant superiority of DL approach in accuracy and efficiency compared to traditional algorithms. It can be expected that using DL to directly extract features from the data may be more effective in detecting earthquake-related ULF anomalies.

V. Conclusion

In this study, we employ a multireference station data-quality-weighting method to explore the ULF geomagnetic precursory phenomena associated with the great Tohoku-Oki earthquake. The detection result reveals a distinctive anomaly

occurring approximately two months prior to the megathrust event. To demonstrate the reliability and robustness of our detection result, we have carried out a comparative analysis against the single-reference station method.

In a thorough investigation of the characteristics and possible mechanisms of the detected anomaly, we carry out a significance test to confirm that the anomaly is not a random occurrence but statistically significant. In addition, by excluding the impact of global magnetic storms, we show that the anomaly was unrelated to external field perturbations due to solar activity. The spatial variation characteristics indicate a concentration of the anomaly energy around the epicenter of the Tohoku-Oki earthquake and a diminishing trend with increasing epicentral distance, further demonstrating the connection between the ULF anomaly and the seismogenic process. Our findings contribute to improving the understanding of the coupling between the ULF electromagnetic phenomena and the earthquake preparation process and demonstrate the tremendous potential of the ULF phenomena as a reliable precursor for earthquake disaster prevention.

ACKNOWLEDGMENT

The authors are grateful to the Geospatial Information Authority of Japan, Japan Meteorological Agency, and Peng Han of the Department of Earth and Space Sciences, Southern University of Science and Technology, for providing geomagnetic data. In addition, they appreciate German Research Centre for Geosciences for supplying the geomagnetic Kp index.

REFERENCES

[1] E. Samardjieva, "Estimation of the expected number of casualties caused by strong earthquakes," *Bull. Seismological Soc. Amer.*, vol. 92, no. 6, pp. 2310–2322, Aug. 2002.

[2] K. D. Marano, D. J. Wald, and T. I. Allen, "Global earthquake casualties due to secondary effects: A quantitative analysis for improving rapid loss analyses," *Natural Hazards*, vol. 52, no. 2, pp. 319–328, Feb. 2010.

[3] K. Goto, T. Ishizawa, Y. Ebina, F. Imamura, S. Sato, and K. Udo, "Ten years after the 2011 Tohoku-oki earthquake and tsunami: Geological and environmental effects and implications for disaster policy changes," *Earth-Sci. Rev.*, vol. 212, Jan. 2021, Art. no. 103417.

[4] S. Uyeda, T. Nagao, and M. Kamogawa, "Short-term earthquake prediction: Current status of seismo-electromagnetics," *Tectonophysics*, vol. 470, nos. 3–4, pp. 205–213, May 2009.

[5] R. Bürgmann, "Reliable earthquake precursors?" *Science*, vol. 381, no. 6655, pp. 266–267, Jul. 2023.

[6] E. E. Papadimitriou, F. F. Evison, D. A. Rhoades, V. G. Karakostas, R. Console, and M. R. Murru, "Long-term seismogenesis in Greece: Comparison of the evolving stress field and precursory scale increase approaches," *J. Geophys. Res., Solid Earth*, vol. 111, no. B5, May 2006, Art. no. B05318.

[7] G. A. Sobolev, "Seismicity dynamics and earthquake predictability," *Natural Hazards Earth Syst. Sci.*, vol. 11, no. 2, pp. 445–458, Feb. 2011.

[8] P. Varotsos and K. Alexopoulos, "Physical properties of the variations of the electric field of the Earth preceding earthquakes, I," *Tectonophysics*, vol. 110, nos. 1–2, pp. 73–98, Dec. 1984.

[9] P. Varotsos and K. Alexopoulos, "Physical properties of the variations of the electric field of the Earth preceding earthquakes. II. Determination of epicenter and magnitude," *Tectonophysics*, vol. 110, nos. 1–2, pp. 99–125, Dec. 1984.

[10] S. Uyeda, T. Nagao, Y. Orihara, T. Yamaguchi, and I. Takahashi, "Geoelectric potential changes: Possible precursors to earthquakes in Japan," *Proc. Nat. Acad. Sci. USA*, vol. 97, no. 9, pp. 4561–4566, Apr. 2000.

[11] P. Varotsos and M. Lazaridou, "Latest aspects of earthquake prediction in Greece based on seismic electric signals," *Tectonophysics*, vol. 188, nos. 3–4, pp. 321–347, Mar. 1991.

[12] P. Varotsos, K. Alexopoulos, and M. Lazaridou, "Latest aspects of earthquake prediction in Greece based on seismic electric signals, II," *Tectonophysics*, vol. 224, nos. 1–3, pp. 1–37, Aug. 1993.

[13] P. Varotsos, K. Alexopoulos, M. Lazaridou-Varotsou, and T. Nagao, "Earthquake predictions issued in Greece by seismic electric signals since February 6, 1990," *Tectonophysics*, vol. 224, nos. 1–3, pp. 269–288, Aug. 1993.

[14] P. A. Varotsos, *The Physics of Seismic Electric Signals*. Tokyo, Japan: TerraPub, 2005.

[15] P. Varotsos, N. Sarlis, and E. Skordas, *Natural Time Analysis: The New View of Time, Part II: Advances in Disaster Prediction Using Complex Systems*. Cham, Switzerland: Springer Nature, 2023.

[16] L. Conti, P. Picozza, and A. Sotgiu, "A critical review of ground based observations of earthquake precursors," *Frontiers Earth Sci.*, vol. 9, p. 528, Jul. 2021.

[17] H. Chen, P. Han, and K. Hattori, "Recent advances and challenges in the seismo-electromagnetic study: A brief review," *Remote Sens.*, vol. 14, no. 22, p. 5893, Nov. 2022.

[18] A. K. Saraf et al., "Satellite detection of earthquake thermal infrared precursors in Iran," *Natural Hazards*, vol. 47, no. 1, pp. 119–135, Oct. 2008.

[19] Y. Zhang and Q. Meng, "A statistical analysis of TIR anomalies extracted by RSTs in relation to an earthquake in the Sichuan area using MODIS LST data," *Natural Hazards Earth Syst. Sci.*, vol. 19, no. 3, pp. 535–549, Mar. 2019.

[20] N. Genzano, C. Filizzola, K. Hattori, N. Pergola, and V. Tramutoli, "Statistical correlation analysis between thermal infrared anomalies observed from MTSATs and large earthquakes occurred in Japan (2005–2015)," *J. Geophys. Res., Solid Earth*, vol. 126, no. 2, Feb. 2021, Art. no. e2020JB020108.

[21] G. A. Sobolev, Q. Huang, and T. Nagao, "Phases of earthquake's preparation and by chance test of seismic quiescence anomaly," *J. Geodynamics*, vol. 33, nos. 4–5, pp. 413–424, May 2002.

[22] Q. Huang and T. Nagao, "Seismic quiescence before the 2000 M= 7.3 Tottori earthquake," *Geophys. Res. Lett.*, vol. 29, no. 12, pp. 19-1–19-41, Jun. 2002.

[23] Q. Huang and X. Ding, "Spatiotemporal variations of seismic quiescence prior to the 2011 M 9.0 Tohoku earthquake revealed by an improved region-time-length algorithm," *Bull. Seismol. Soc. Amer.*, vol. 102, no. 4, pp. 1878–1883, Aug. 2012.

[24] Y. Zeng, M. D. Petersen, and Z. Shen, "Earthquake potential in California–Nevada implied by correlation of strain rate and seismicity," *Geophys. Res. Lett.*, vol. 45, no. 4, pp. 1778–1785, Feb. 2018.

[25] G. Zhao et al., "A review of seismo-electromagnetic research in China," *Sci. China Earth Sci.*, vol. 65, no. 7, pp. 1229–1246, Jul. 2022.

[26] M. Hayakawa, A. Schekotov, J. Izutsu, A. P. Nickolaenko, and Y. Hobara, "Seismogenic ULF/ELF wave phenomena: Recent advances and future perspectives," *Open J. Earthq. Res.*, vol. 12, no. 3, pp. 45–113, 2023.

[27] M. Fedi, M. La Manna, and F. Palmieri, "Nonstationary analysis of geomagnetic time sequences from Mount Etna and North Palm Springs earthquake," *J. Geophys. Res., Solid Earth*, vol. 108, no. B10, p. 2493, Oct. 2003.

[28] K. Hattori et al., "ULF geomagnetic anomaly associated with 2000 Izu Islands earthquake swarm, Japan," *Phys. Chem. Earth*, vol. 29, nos. 4–9, pp. 425–435, Jan. 2004.

[29] P. Han, Q. Huang, and J. Xiu, "Principal component analysis of geomagnetic diurnal variation associated with earthquakes: Case study of the M6.1 Iwate-ken Nairiku Hokubu earthquake," *Chin. J. Geophys.*, vol. 52, no. 6, pp. 1556–1563, 2009.

[30] Q. Huang, "Retrospective investigation of geophysical data possibly associated with the Ms8.0 Wenchuan earthquake in Sichuan, China," *J. Asian Earth Sci.*, vol. 41, nos. 4–5, pp. 421–427, Jun. 2011.

[31] K. Hattori, P. Han, C. Yoshino, F. Febriani, H. Yamaguchi, and C.-H. Chen, "Investigation of ULF seismo-magnetic phenomena in Kanto, Japan during 2000–2010: Case studies and statistical studies," *Surv. Geophys.*, vol. 34, no. 3, pp. 293–316, May 2013.

[32] P. Han et al., "Statistical analysis of ULF seismomagnetic phenomena at Kakioka, Japan, during 2001–2010," *J. Geophys. Res., Space Phys.*, vol. 119, no. 6, pp. 4998–5011, Jun. 2014.

[33] F. Febriani et al., "Ultra low frequency (ULF) electromagnetic anomalies associated with large earthquakes in Java island, Indonesia by using wavelet transform and detrended fluctuation analysis," *Natural Hazards Earth Syst. Sci.*, vol. 14, no. 4, pp. 789–798, Apr. 2014.

[34] P. Han, K. Hattori, J. Zhuang, C.-H. Chen, J.-Y. Liu, and S. Yoshida, "Evaluation of ULF seismo-magnetic phenomena in Kakioka, Japan by using Molchan's error diagram," *Geophys. J. Int.*, vol. 208, no. 1, pp. 482–490, Jan. 2017.

[35] P. Han et al., "Assessing the potential earthquake precursory information in ULF magnetic data recorded in Kanto, Japan during 2000–2010: Distance and magnitude dependences," *Entropy*, vol. 22, no. 8, p. 859, Aug. 2020.

[36] W. D. Heavlin et al., "Case-control study on a decade of ground-based magnetometers in California reveals modest signal 24–72 hr prior to earthquakes," *J. Geophys. Res., Solid Earth*, vol. 127, no. 10, Oct. 2022, Art. no. e2022JB024109.

[37] K. A. Yusof, M. Abdullah, N. S. A. Hamid, S. Ahadi, and E. Ghamry, "Statistical global investigation of pre-earthquake anomalous geomagnetic diurnal variation using superposed epoch analysis," *IEEE Trans. Geosci. Remote Sens.*, vol. 60, 2022, Art. no. 2001413.

[38] K. Hattori, "ULF geomagnetic changes associated with large earthquakes," *Terr., Atmos. Ocean. Sci.*, vol. 15, no. 3, pp. 329–360, 2004.

[39] X. Liu, K. Hattori, P. Han, H. Chen, Y. Chie, and X. Zhao, "Possible anomalous changes in solar quiet daily geomagnetic variation (Sq) related to the 2011 off the Pacific coast of Tohoku earthquake (Mw 9.0)," *Pure Appl. Geophys.*, vol. 177, no. 1, pp. 333–346, Jan. 2020.

[40] Y. Orihara, M. Kamogawa, and T. Nagao, "Preseismic changes of the level and temperature of confined groundwater related to the 2011 Tohoku earthquake," *Sci. Rep.*, vol. 4, no. 1, p. 6907, Nov. 2014.

[41] T. Nagao, Y. Orihara, and M. Kamogawa, "Precursory phenomena possibly related to the 2011 M 9.0 off the Pacific coast of Tohoku earthquake," *J. Disaster Res.*, vol. 9, no. 3, pp. 303–310, Jun. 2014.

[42] N. V. Sarlis et al., "Minimum of the order parameter fluctuations of seismicity before major earthquakes in Japan," *Proc. Nat. Acad. Sci. USA*, vol. 110, no. 34, pp. 13734–13738, Aug. 2013.

[43] P. A. Varotsos, N. V. Sarlis, and E. S. Skordas, "Phenomena preceding major earthquakes interconnected through a physical model," *Annales Geophysicae*, vol. 37, no. 3, pp. 315–324, May 2019.

[44] P. A. Varotsos, N. V. Sarlis, E. S. Skordas, T. Nagao, and M. Kamogawa, "Natural time analysis together with non-extensive statistical mechanics shorten the time window of the impending 2011 Tohoku M9 earthquake in Japan," *Commun. Nonlinear Sci. Numer. Simul.*, vol. 125, Oct. 2023, Art. no. 107370.

[45] G. Xu, P. Han, Q. Huang, K. Hattori, F. Febriani, and H. Yamaguchi, "Anomalous behaviors of geomagnetic diurnal variations prior to the 2011 off the Pacific coast of Tohoku earthquake (Mw9.0)," *J. Asian Earth Sci.*, vol. 77, pp. 59–65, Nov. 2013.

[46] P. Han et al., "Further investigations of geomagnetic diurnal variations associated with the 2011 off the Pacific coast of Tohoku earthquake (Mw 9.0)," *J. Asian Earth Sci.*, vol. 114, pp. 321–326, Dec. 2015.

[47] P. Han, K. Hattori, Q. Huang, S. Hirooka, and C. Yoshino, "Spatiotemporal characteristics of the geomagnetic diurnal variation anomalies prior to the 2011 Tohoku earthquake (Mw 9.0) and the possible coupling of multiple pre-earthquake phenomena," *J. Asian Earth Sci.*, vol. 129, pp. 13–21, Nov. 2016.

[48] R. T. Merrill, M. W. McElhinny, and P. L. McFadden, *The Magnetic Field of the Earth*. San Diego, CA, USA: Academic Press, 1996.

[49] R. Lanza and A. Meloni, *The Earth's Magnetic Field*. Berlin, Germany: Springer, 2006.

[50] J. Y. Liu, C. H. Chen, Y. I. Chen, H. Y. Yen, K. Hattori, and K. Yumoto, "Seismo-geomagnetic anomalies and M $\geq$ 5.0 earthquakes observed in Taiwan during 1988–2001," *Phys. Chem. Earth*, vol. 31, nos. 4–9, pp. 215–222, 2006.

[51] C.-H. Chen et al., "Pre-seismic geomagnetic anomaly and earthquake location," *Tectonophysics*, vol. 489, nos. 1–4, pp. 240–247, Jun. 2010.

[52] D. F. Mix and K. J. Olejniczak, *Elements of Wavelets for Engineers and Scientists*. Hoboken, NJ, USA: Wiley, 2003.

[53] A. Gvishiani and A. Soloviev, *Observations, Modeling and Systems Analysis in Geomagnetic Data Interpretation*. Cham, Switzerland: Springer, 2020.

[54] P. Varotsos, N. Sarlis, and E. Skordas, "Order parameter and entropy of seismicity in natural time before major earthquakes: Recent results," *Geosciences*, vol. 12, no. 6, p. 225, May 2022.

[55] L. B. Mohr, *Understanding Significance Testing*. London, U.K.: Sage, 1990.

[56] P. Varotsos, "Spatio-temporal complexity aspects on the interrelation between seismic electric signals and seismicity," *Pract. Athens Acad.*, vol. 76, pp. 294–321, Jan. 2001.

[57] N. V. Sarlis, E. S. Skordas, P. A. Varotsos, T. Nagao, M. Kamogawa, and S. Uyeda, "Spatiotemporal variations of seismicity before major earthquakes in the Japanese area and their relation with the epicentral locations," *Proc. Nat. Acad. Sci. USA*, vol. 112, no. 4, pp. 986–989, Jan. 2015.

[58] Y. LeCun, Y. Bengio, and G. Hinton, "Deep learning," *Nature*, vol. 521, no. 7553, pp. 436–444, May 2015.

[59] I. Goodfellow, Y. Bengio, and A. Courville, *Deep Learning*. Cambridge, MA, USA: MIT Press, 2016.

[60] S. Yu and J. Ma, "Deep learning for geophysics: Current and future trends," *Rev. Geophys.*, vol. 59, no. 3, Sep. 2021, Art. no. e2021RG000742.

[61] S. M. Mousavi and G. C. Beroza, "Deep-learning seismology," *Science*, vol. 377, no. 6607, pp. 725–736, Aug. 2022.

[62] J. Xue, Q. Huang, S. Wu, and T. Nagao, "LSTM-autoencoder network for the detection of seismic electric signals," *IEEE Trans. Geosci. Remote Sens.*, vol. 60, 2022, Art. no. 5917012.

[63] J. Xue, S. Wu, Q. Huang, L. Zhao, N. V. Sarlis, and P. A. Varotsos, "RASE: A real-time automatic search engine for anomalous seismic electric signals in geoelectric data," *IEEE Trans. Geosci. Remote Sens.*, vol. 61, 2023, Art. no. 5905911.

Jiyan Xue received the B.S. degree in geophysics from China University of Geosciences, Wuhan, China, in 2020. He is currently pursuing the Ph.D. degree with the Department of Geophysics, Peking University, Beijing, China, under the supervision of Prof. Q. Huang.

His research interests include electromagnetic data processing, radar signal inversion, and deep learning.

Qinghua Huang received the Ph.D. degree in physics from Osaka University, Osaka, Japan, in 1999.

He is currently a Professor in geophysics, Peking University, Beijing, China. His research focuses on the development and application of geoelectromagnetic methods.

Sihong Wu received the Ph.D. degree in solid geophysics from Peking University, Beijing, China, in 2021, followed by a two-year post-doctoral program at the same institution.

She is currently a Post-Doctoral Fellow with the Department of Earth and Atmospheric Sciences, University of Houston, Houston, TX, USA. Her research interests include airborne electromagnetic data analysis, marine magnetic anomaly detection, magnetization inversion, and deep learning.

Li Zhao received the Ph.D. degree in geophysics from Princeton University, Princeton, NJ, USA, in 1995.

He is currently a Chair Professor with Peking University, Beijing, China, where he is also the Director of the Institute of Theoretical and Applied Geophysics, School of Earth and Space Sciences. He has published more than 100 articles in professional journals. His research focuses on the development and application of full-waveform seismic tomography.

Dr. Zhao is an Associate Editor of the *Journal of Geophysical Research: Solid Earth*.